



*Dedicated to Nicolae I. Ionescu PhD  
on the occasion of his 85th anniversary*

## TUNGSTEN-MODIFIED HMS CATALYSTS FOR HIGH SELECTIVE OXIDATION OF STYRENE WITH AQUEOUS HYDROGEN PEROXIDE

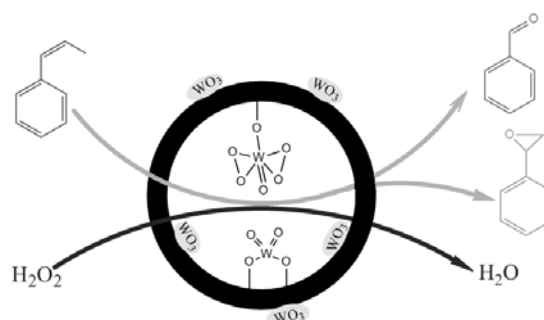
Viorica PARVULESCU,<sup>a,\*</sup> Madalina CIOBANU,<sup>a</sup> Gabriela PETCU,<sup>a</sup>  
Elena Maria ANGHEL<sup>a</sup> and Bao-Lian SU<sup>b</sup>

<sup>a</sup>“Ilie Murgulescu” Institute of Physical Chemistry, Roumanian Academy, Splaiul Independenței 202, 060021, Bucharest, Roumania

<sup>b</sup>Laboratoire de Chimie des Matériaux Inorganiques, The University of Namur (FUNDP),  
61 rue de Bruxelles, B-5000 Namur, Belgium

*Received July 31, 2017*

Tungsten-modified HMS catalysts were obtained following the oxo-peroxo and oxo-polyoxo routes by microwave heating method in presence of cetyltrimethylammonium chloride or cetylpyridine chloride as surfactants. The obtained materials were characterized by XRD, N<sub>2</sub> adsorption/desorption, SEM, TEM, FTIR and Raman spectroscopy. XRD patterns at small angle exhibit a peak with differences in intensity of the reflections, significantly influenced by the method and variables of the synthesis. A typical wormhole-like pore structure of W-HMS materials, with network channels and uniform pore sizes, was observed by TEM images. The obtained tungsten-silicates were active in oxidation with hydrogen peroxide of the hydrocarbons with double bonds as styrene. The best results were obtained for the catalysts synthesized by oxo-polyoxo route, with ordered porous structure, high surface area and lower Si/W molar ratio.



### INTRODUCTION

Oxidation is one of the main used reactions in converting of petroleum-based materials, in fine chemistry or degradation of organic pollutants. In the latest time, green synthesis methods of catalysts and environmentally friendly processes that are using oxidants such as air, oxygen or hydrogen peroxide are preferred.<sup>1-3</sup> The use of hydrogen peroxide in oxidation of organic substrates generates various types of products depending on the catalysts used and

the reaction conditions. Thus, the oxidation of styrene with hydrogen peroxide is of interest for the synthesis of two important products— styrene oxide and benzaldehyde.<sup>4</sup> Many of the catalysts used in these applications have been obtained by generating of catalytic active sites in mesoporous silicas.<sup>5-10</sup> The discovery of mesoporous silica materials has opened new possibilities in the development of catalysts by green synthesis methods. The introduction of redox transitional metal ions into mesoporous oxide matrices has been proposed as an interesting way to

\* Corresponding author: [vpirvulescu@icf.ro](mailto:vpirvulescu@icf.ro)

produce oxidation catalysts. Owing to their large surface area, ordered porous structure and narrow pore distribution, they were used as hosts at creating novel composite materials and tailoring the catalytic properties by incorporation of transition metals such as V, Co, Cr, Mn, Fe, Ni.<sup>5,7</sup> These materials are usually prepared by direct synthesis and hydrothermal treatment. However, in the latest years an alternative method appeared known as microwave heating.<sup>11</sup> This method is a rapid and efficient way to control the nucleation, particle size, distribution and macroscopic morphology of mesostructured materials.

The incorporation of tungsten into the mesoporous silica framework remains a challenge, due to the large diameter of the tungsten atom and its high oxidation state. Up to date, some tungsten-containing mesoporous materials were used, such as W-MCM-48,<sup>12,13</sup> W-SBA-15<sup>14-16</sup> and W-MCM-41.<sup>17,18</sup> Incorporation of such large species into the silica framework is hindered and the formation of extra framework tungsten oxide could be favoured.

Regarding the incorporation of tungsten species into the MCM-41 framework, there is a critical value for the Si/W ratio of about 30. In the case of smaller Si/W ratio, the formation of extra framework tungsten oxide species is observed.<sup>19,20</sup> W- modified mesoporous silicas were reported as heterogeneous catalysts for selective oxidation of olefins with aqueous solution of H<sub>2</sub>O<sub>2</sub>.<sup>21,22</sup> The structure and catalytic properties of supported tungsten oxide are strongly influenced by the support. On the other hand, this oxide is sensitive

to the intrinsic nature of the tungsten species, including oxidation state, coordination circumstance, dispersion, and stability.<sup>16</sup>

In this paper we report the incorporation, by direct synthesis, of tungsten species into hexagonal mesoporous silica (HMS), a promising catalytic support. The obtained redox molecular sieves were tested in oxidation of styrene with hydrogen peroxide. The influence of the synthesis parameters, such as, chemical composition of the gels, surfactant, precursors and time of the hydrothermal treatment, on the structure, morphology, nature of metal species and catalytic properties has been examined.

## RESULTS AND DISCUSSION

X-Ray patterns at low angle of WM1-5 samples (Fig 1), obtained by oxo-peroxo mode, show only a peak at small angle with low intensity for samples WM1 and WM2. We consider that is the result of lower CTAC/Si(OR)<sub>4</sub> molar ratio (0.1) used in synthesis of WM2-4 samples. The intensity of this peak is significantly higher for sample WM5 obtained in conditions of higher CTAC/Si(OR)<sub>4</sub> molar ratio (0.3). All X-Ray patterns of samples obtained by oxo-polyoxo method in conditions of higher surfactant/Si(OR)<sub>4</sub> molar ratio (0.3-WM7-12) show a X-ray reflection at low angle (2θ~2.8°), arising from the hexagonal array of silica tubes of HMS (Fig. 1).

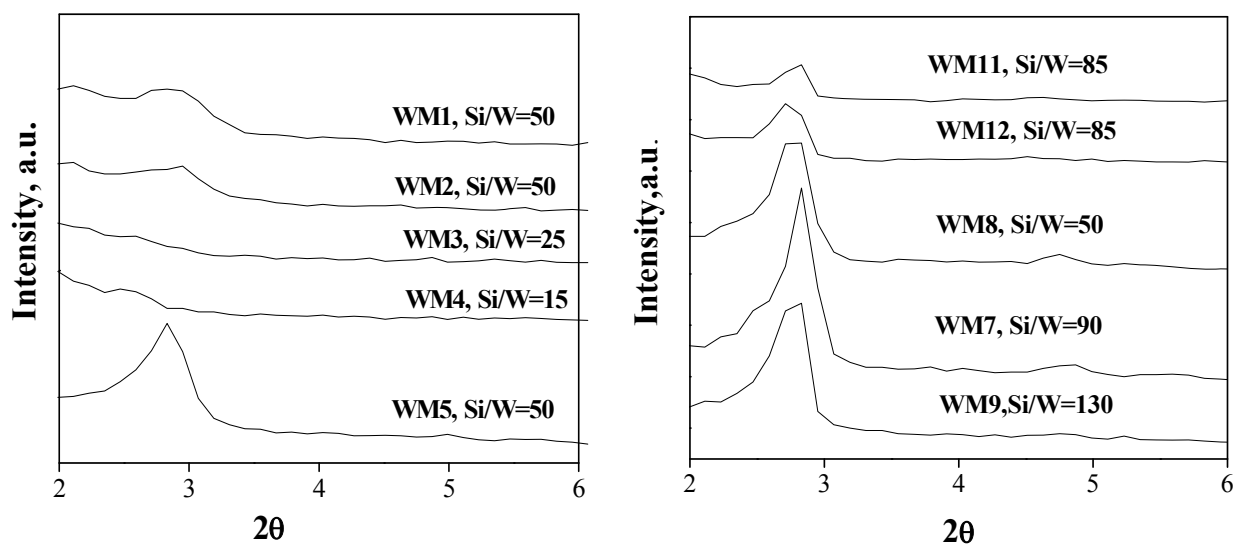


Fig. 1 – XRD patterns of W-HMS samples.

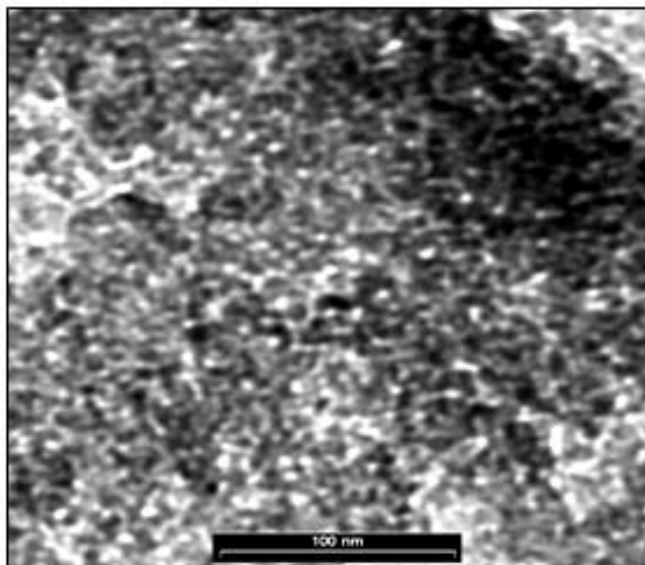


Fig. 2 – TEM image of WM12 sample.

Table 1

Conditions of the synthesis, characteristics of porous structure and activity

Sample	Si/W	Surfactant	Synth. Method	Hydroth. Time (h)	$S_{\text{BET}}$ , ( $\text{m}^2\text{g}$ )	$\Phi$ , (nm)	C, (%)	TOF, ( $\text{h}^{-1}$ )
WM1	50	CTAC	1	2	790	2.3	42.5	0.9
WM6	90	CPC	2	2	965	2.3	52.6	1.5
WM7	90	CPC	2	1	940	2.1	53.6	1.6
WM8	50	CPC	2	2	1100	2.0	64.1	2.2
WM9	130	CPC	2	2	950	2.1	48.6	1.2
WM11	85	CPC	2	2	980	2.2	54.8	1.8
WM12	85	CPC	2	4	870	2.4	46.8	1.0

Reaction time: 24 h, reaction temperature: 323K, TOF: moles of styrene converted per mole of  $\text{WO}_3$  calculated in the catalyst per hour.

HMS materials also belong to the family of mesoporous silicas but show important differences when compared to MCM-41 solids.<sup>23</sup> In particular, they are characterized by a lower degree of long range ordering, a higher textural porosity and smaller pore sizes. The differences in intensity of the reflections, evidenced by X-Ray diffraction (Figures 1), surface area and pore size are significantly influenced by the method and variables of the synthesis (Table 1). Thus, the higher intensity of the (100) peak was obtained for samples obtained by oxo-polyoxo mode in presence of CPC as surfactant (WM6-12) and lower time of the microwave heating (WM7). The optimal surfactant/ $\text{Si}(\text{OR})_4$  molar ratio was 0.3. Any peak was obtained by XRD for sample WM10 hydrothermal treated 1h at 60°C and a similar diffractogram with WM7 sample was obtained for WM6 catalyst.

A typical wormhole-like pore structure of W-HMS materials, with network channels and uniform pore sizes, was observed in TEM images (Fig. 2). The morphology of the samples is presented in Fig. 3.

In conditions of low surfactant/ $\text{Si}(\text{OR})_4$  molar ratio, arrangements of particles with different forms were obtained (Fig. 3a). At higher molar ratios particles with spherical morphology were obtained (Fig. 3d). SEM images of samples obtained in conditions of higher surfactant/ $\text{Si}(\text{OR})_4$  molar ratio show two different morphologies (Figs. 3b, 3c, 3d). For example, WM10 sample shows a morphology of typical fiber and co-existing spherical particles (Fig. 3c) comparing to WM5 sample when gyroids were obtained (Fig. 3b).

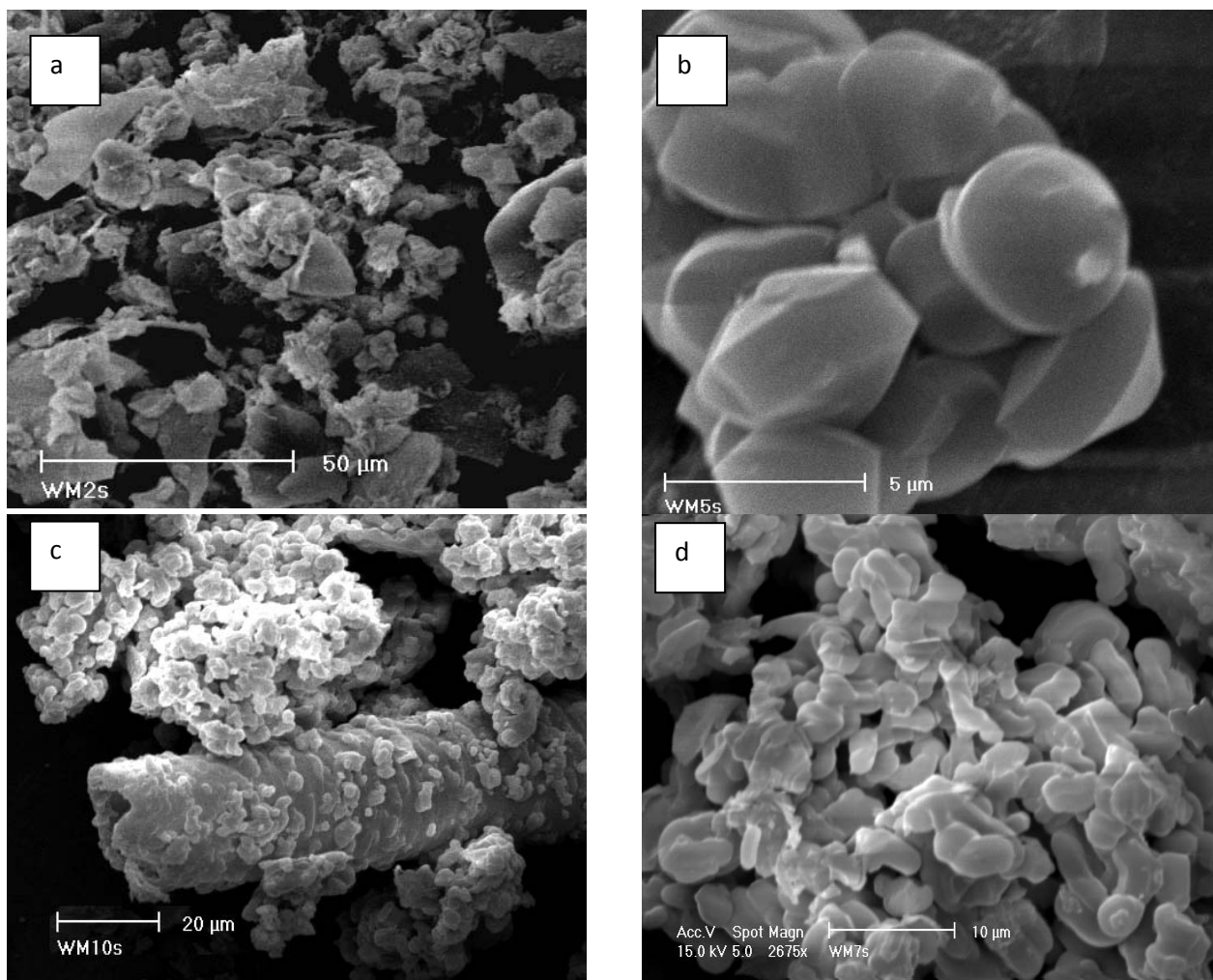


Fig. 3 – SEM images of the samples obtained by oxo-peroxo route in conditions of various CTAC/Si(OR)<sub>4</sub> molar ratio (a-0.1; b-0.3) and oxo-polyoxo route in conditions of different temperature of the hydrothermal treatment (c-60°C; d-80°C).

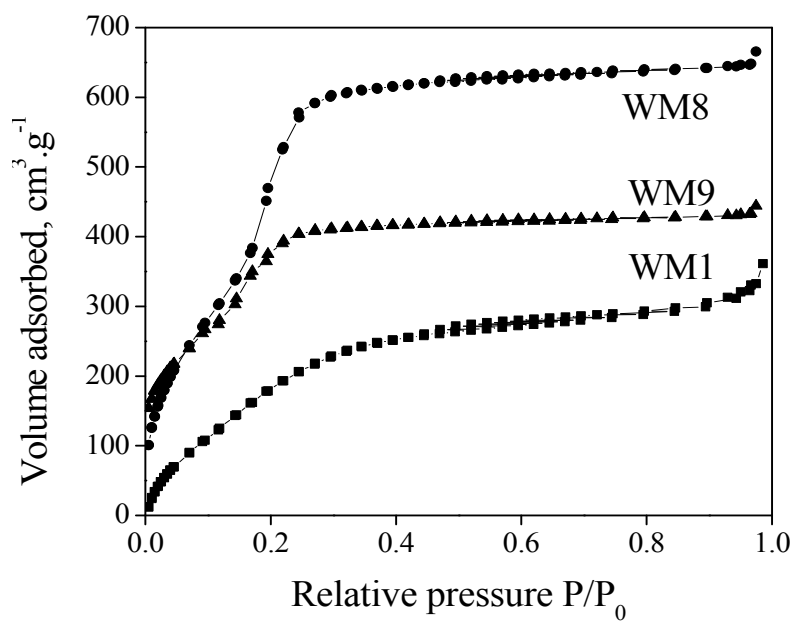


Fig. 4 – N<sub>2</sub> adsorption-desorption isotherms.

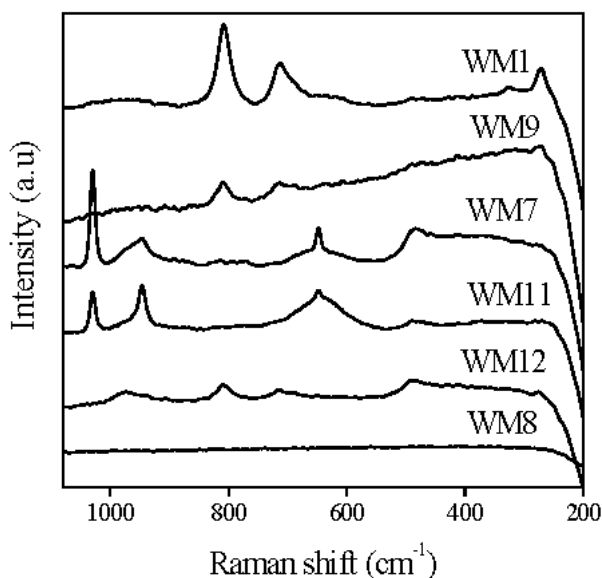


Fig. 5 – Raman spectra of the obtained samples with various Si/W molar ratios.

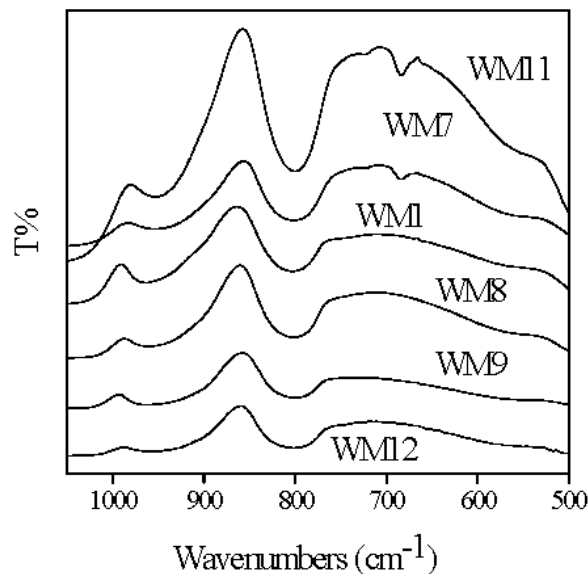
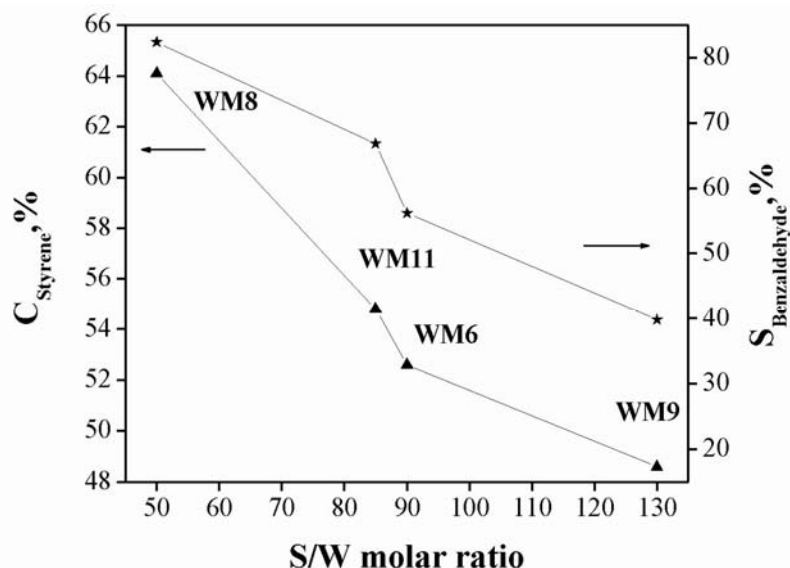


Fig. 6 – FTIR spectra of the obtained samples.

Fig. 7 – Variation of conversion and selectivity with Si/W molar ratio.



The nitrogen adsorption-desorption isotherms confirm the significant effect of the synthesis route and Si/W molar ratio on the pore volume (Fig. 4). All the materials exhibit a type IV isotherm and a sharp inflection point characterizing the capillary condensation within the mesopores ( $P/P_0 = 0.2-0.3$ ). For the samples synthesized by route 2 it was found that the surface area is higher (Table 1). The highest surface area was obtained in condition of 2 h time of the hydrothermal heating and Si/W=50 molar ratio (WM8).

Nature of tungsten species was studied by Raman and FTIR spectra of the obtained samples. These spectra detected peroxo and polyoxo

tungsten vibrations. Raman spectra of the samples are shown in Fig. 5.

Samples WM1 and WM9, synthesized by route 1 respectively 2 with higher Si/W molar ratio in each group, show sharp bands characteristic for  $\text{WO}_6$  groups in the  $\text{WO}_3$  oxide (about 809, 719 and 270  $\text{cm}^{-1}$  corresponding to W-O-W deformation mode, W-O bending mode and symmetric stretching mode of W-O) which is a strong Raman scatterer and hence can mask other spectral features. These Raman bands reflect the high dispersion of the tungsten oxide phase on the  $\text{SiO}_2$  support under hydrated and dehydrated conditions.<sup>24,25</sup> The band and/or shoulder at

$\sim 970\text{ cm}^{-1}$  of the WM7, WM11 and WM12 samples was assigned to the vibration of the isolated  $[\text{WO}_4]^{2-}$  and surface  $\equiv\text{Si-OH}$  species whereas those at  $480\text{ cm}^{-1}$  were associated with vibrations of the siloxane rings.<sup>22,24,26</sup> Raman spectra of WM8 sample are typically for W-hexagonal mesoporous silica<sup>19</sup>, while mostly of its tungsten ions in sample WM8—should occur as isolated or low condensed oligomeric framework species. Therefore, in the obtained samples tungsten species on the surface are as  $\text{WO}_3$  oxide (samples WM1, WM9 and WM12) and as single-site  $[\text{WO}_4]^{2-}$  species bound strongly to silica through W–O–Si covalent bonds (samples WM7, WM11, WM12). Raman features corresponding to the peroxo moieties at  $854$ ,  $638$  and  $564\text{ cm}^{-1}$  were reported in literature as assignable to O–O, asymmetric and symmetric  $\text{W}(\text{O}_2)$  vibrations, the  $[\text{R}_2\text{SiO}_2\{\text{W}_2\text{O}_2(\mu\text{-O}_2)_2(\text{O}_2)_2\}]^{2-}$  and  $[\text{R}_3\text{SiO}\{\text{WO}(\text{O}_2)_2\}]^-$  anions<sup>27</sup>. Although band located around  $640\text{ cm}^{-1}$  might belong to asymmetric  $\text{W}(\text{O}_2)$  modes no band due to the O–O vibration modes at  $\sim 850\text{ cm}^{-1}$  was evidenced in Raman spectra for the WM7 and WM11, WM12 samples. Conversely, the band located at  $1029\text{ cm}^{-1}$  indicated presence of the W=O linkages within the surface  $\text{WO}_x$  species.<sup>26</sup> Any W species were evidenced by Raman spectroscopy for the WM8 sample as result of a very high dispersion of isolated W sites on a highest surface.

The FTIR spectra in the wavenumber range  $1100\text{--}500\text{ cm}^{-1}$  of W-HMS mesoporous materials with different W contents are presented in Fig.6. All the materials exhibited two characteristic bands at around  $1000$  and  $800\text{ cm}^{-1}$  caused by the presence of Si–O–Si vibrations characteristic peaks of silica-based mesostructure. The first band was assigned to the asymmetric  $\nu_{\text{asym}}(\text{Si-O-Si})$ , whereas the second was attributed to a symmetric  $\nu_{\text{sym}}(\text{Si-O-Si})$  stretching vibration and the bending modes of the  $\text{SiO}_4$  tetrahedra vibrations.<sup>20,28</sup> The FT-IR spectra of the W-HMS materials retained the typical IR absorption characteristics of HMS support, indicating the materials were in the typical mesoporous structure of HMS. As a consequence of the incorporation of tungsten into hexagonal mesoporous silica, Si–O–Si vibrational bands shift to lower values of wave number. In FTIR spectra of WM samples the vibration band around  $960\text{ cm}^{-1}$  may be assigned to W–O–Si linkage.

The obtained tungsten-silicates are active in oxidation of styrene with hydrogen peroxide. The best results were obtained for the catalysts synthesized by route 2, with ordered porous

structure, lower Si/W molar ratio and higher surface area (Table 1, Fig. 7). A significant difference between catalytic activity of the samples with similar Si/W molar ratio (samples WM1 and WM8) suggests that the synthesis route influences the nature of tungsten species and their dispersion on or in the silica matrix. The catalysts with more ordered structure, higher surface area and  $[\text{WO}_4]^{2-}$  species strongly bounded or high dispersed on silica have a higher activity.

Conversion and selectivity to benzaldehyde decreased with Si/W molar ratio. In Fig. 7 are presented these results for samples obtained by route 2 in condition of 2 h of hydrothermal treatment. The highest conversion of styrene to benzaldehyde has been evidenced for WM8 sample with the highest amount of isolated W sites and surface area.

## EXPERIMENTAL

### 1. Materials

Tetraethyl orthosilicate (TEOS) and tetramethyl orthosilicate (TMOS) silica sources,  $\text{WO}_3\cdot\text{H}_2\text{O}$  and  $\text{Na}_2\text{WO}_4\cdot 2\text{H}_2\text{O}$  as tungsten sources, cetyltrimethylammonium chloride (CTAC) and cetylpyridine chloride (CPC) surfactants and the reactants (styrene and peroxide solution-30%) were purchased from Sigma Aldrich. All chemicals used in this work were of analytical grade and were used without any further purification.

### 2. Preparation of catalysts

Mesoporous tungsteno-silicates (WM1-12 samples) were prepared following the oxo-peroxo synthesis:  $[\text{WO}_4]^{2-}/\text{H}_2\text{O}/\text{H}_3\text{O}^+$ /surfactant/ $\text{Si}(\text{OR})_4$  (route 1) and oxo-polyoxo mode:  $[\text{WO}(\text{O}_2)_2(\text{H}_2\text{O})_2]/\text{H}_2\text{O}/\text{H}_3\text{O}^+$ /surfactant/ $\text{Si}(\text{OR})_4$  (route 2). WM1-5 samples were obtained by route 1 with CTAC as surfactant. CTAC/ $\text{SiO}_2$  molar ratio was 0.1, for WM1-4 samples, and 0.3 for WM5. Si/W molar ratio varied between 15 and 50. WM6-12 samples were obtained by route 2 with CPC as surfactant and Si/W molar ratio between 50 and 130. The  $\text{Si}(\text{OR})_4$  precursors were TEOS (WM1, WM6) and TMOS. In the first step of each synthesis the surfactant was introduced into aqueous solution of HCl and stirred for one hour. Finally silica and tungsten sources were introduced under stirring and the obtained mixtures were hydrothermal treated for 1h (WM7, WM8), 2h (WM1-5, WM1-6, WM9-11) and 4 h (WM12) by microwave heating method. The obtained materials were dried and calcined at  $550\text{ }^\circ\text{C}$  in air.

### 3. Characterisation

Powder X-ray diffraction (XRD) measurements were performed on a Bruker AXS D8 diffractometer and N2 adsorption/desorption isotherms were obtained with a Micromeritics (Tristar) instrument. The morphology and porous structure of the samples were investigated by scanning electron microscopy (FEI Quanta 3D FEG) transmission electron microscopy (Tecnai microscope). FTIR and Raman spectra were recorded by Fourier transform infrared spectrometer (Spectrum -Perkin-Elmer).

#### 4. Measurements of catalytic activity

The obtained samples were tested in oxidation of styrene with hydrogen peroxide. The oxidation reaction was carried out in the thermostated glass reactor with magnetic stirring using acetonitrile as solvent. The reaction temperature was varied between 293–343 K and the time between 2 – 8 h. The molar ratio of styrene/ solvent/hydrogen peroxide was 1/1.8/3. After separation of the catalyst by centrifugation, the analyses of the oxidation products were performed using a DANI 1000 gas chromatograph with FID detector.

### CONCLUSIONS

In conclusion, the method of synthesis and the preparation variables influence the porous structure, morphology and nature of the metal species. The isolates W sites incorporated into mesoporous HMS silica network are active and selective in catalytic oxidation of olefins. The best results were obtained for samples with single-site  $[\text{WO}_4]^{2-}$  species bounded strongly to silica through W–O–Si covalent bonds and very well dispersed.

### REFERENCES

1. S.-Y. Na and Y. Lee, *Catal. Today*, **2017**, 282, 86-94.
2. R. Fareghi-Alamdari, N. Zekri, A. J. Moghadam and M. R. Farsani, *Catal. Commun.*, **2017**, 98, 71-75.
3. G. Liu, J. Ji, H. Huang, R. Xie, Q. Feng, Y. Shu, Y. Zhan, R. Fang, M. He, S. Liu, X. Ye and D.Y.C. Leung, *Chem. Eng. J.*, **2017**, 324, 44-50.
4. W. Tanglumlert, T. Imae, T. J. White and S. Wongkasemjit, *Catal. Commun.*, **2009**, 10, 1070–1073.
5. S. Todorova, V. Parvulescu, G. Kadinov, K. Tenchev, S. Somacescu and B.-L. Su, *Microp. Mesop. Mater.*, **2008**, 113, 22-30.
6. I. D. Ivanchikova, N. V. Maksimchuk, I.Y. Skobelev, V. V. Kaichev and O. A. Kholdeeva, *J. Catal.*, **2015**, 332, 138-148.
7. V. Parvulescu and B. L. Su, *Catal. Today*, **2001**, 69, 315-322.
8. W. Zhan, Y. Guo, Y. Wang, Y. Guo and G. Lu, *J. Rare Earths*, **2010**, 28, 369-375.
9. V. Parvulescu, C. Anastasescu and B.L. Su, *J. Mol. Catal. A: Chem.*, **2004**, 211, 143-148.
10. O. Klepel, W. Bohlmann, E.B. Ivanov, V. Riede and H. Papp, *Micropor. Mesop. Mater.*, **2004**, 76, 105-109.
11. M. Run, S.Wu and G. Wu, *Micropor. Mesop. Mater.*, **2004**, 74, 37-47.
12. X.L. Yang, W.L. Dai, R.H. Gao, H. Chen, H.X. Li, Y. Cao and K.N. Fan, *J. Mol. Catal. A: Chem.*, **2005**, 241, 205–214.
13. D.R. Hua, S.L. Chen, G.M. Yuan and Y.L. Wang, *J. Porous Mater.*, **2011**, 18, 729–734.
14. L. Dimitrov, R. Palcheva, A. Spojakina and K. Jiratova, *J. Porous Mater.*, **2001**, 18, 425–434.
15. J.C. Hu, Y.D. Wang, L.F. Chen, R. Richards, W.M. Yang, Z.C. Liu and W. Xu, *Microp. Mesop. Mater.*, **2006**, 93, 158–163.
16. J. E. Herrera, J. H. Kwak, J. Z. Hu, Y. Wang, C. H.F. Peden, J. Macht and E. Iglés, *J. Catal.*, **2006**, 239, 200–211.
17. H. Chen, W.L. Dai, R.H. Gao, Y. Cao, H.X. Li and K.N. Fan, *Appl. Catal., A*, **2007**, 328, 226–236.
18. O. Klepel, W. Bohlmann, E.B. Ivanov, V. Riede and H. Papp, *Microp. Mesop. Mater.*, **2004**, 76, 105–112.
19. J.-M. Bregeault, J.Y. Piquemal, E. Briot, E. Duprey, F. Launay, L. Salles, M.Vennat and A.-P. Legrand, *Micropor. Mesop. Mater.*, **2001**, 44-45, 409-417.
20. H.-Y. Wu, X.-L. Zhang, C.-Y. Yang, X. Chen and X.-C. Zheng, *Appl. Surf. Sci.*, **2013**, 270, 590–595.
21. H. Chen, W.-L. Dai, J.-F. Deng and K. Fan, *Catal. Lett.*, **2002**, 81, 131-136.
22. R. Gao, X. Yang, W.-L. Dai, Y. Le, H. Li and K. Fan, *J. Catal.*, **2008**, 256, 259-267.
23. M.H. Peyrovi, N. Parsafard and P. Peyrovi, *Ind. Eng. Chem. Res.*, **2014**, 53, 14253–14262.
24. E. I. Ross-Medgaarden and I. E. Wachs, *J. Phys. Chem. C*, **2007**, 111, 15089-15099.
25. Z. Zhang, J. Suo, X. Zhang and S. Li, *Chem. Commun.*, **1998**, 0(2), 241-242.
26. M.P. Pachamuthu, R. Maheswari, A. Ramanathan, *Appl. Surf. Sci.* **2017**, 402, 286-293.
27. J.-Y. Piquemal, E. Briot, G.Chottard, P. Tougne, J.-M. Manoli and J.-M. Bregeault, *Microp. Mesop. Mater.*, **2003**, 58, 279–289.
28. M. Zhang, W. Zhu, H. Li, S. Xun, W. Ding, J. Liu, Z. Zhao, Q. Wang, *Chem. Eng. J.*, **2014**, 243, 386–393.

